Electronic Supplementary Information

**Photoelectrochemical Water Splitting in an Organic Artificial Leaf**

Serkan Esiner, Robin E. M. Willems, Alice Furlan, Weiwei Li, Martijn M. Wienk, and René A. J. Janssen

Contents

1. A larger area organic leaf with earth-abundant catalysts

PEC water splitting with a large area solar cell was also performed with earth-abundant catalysts. A ~1.2 cm^2 triple junction cell was integrated with Co_3O_4/NiMoZn catalysts (~1.0 cm^2 each) in 0.1 M KBi for oxygen and hydrogen evolution reactions. This solar cell had an efficiency of 5.7%, which reduced during the 20 min water splitting experiment (Fig. S1a). The operating voltage for this device was 1.83 V as shown in Fig. S1b. A low J_{op} of 1.03 mA cm^{-2} was observed during water splitting, which resulted in a solar to hydrogen conversion efficiency of 1.27%. The reason for low η_{STH} is partially due to reduced fill factor by degradation of the solar cell and partially due to increased current density on the catalyst surfaces which increased the overpotentials and the operating voltage (Fig. S2 - ◇).
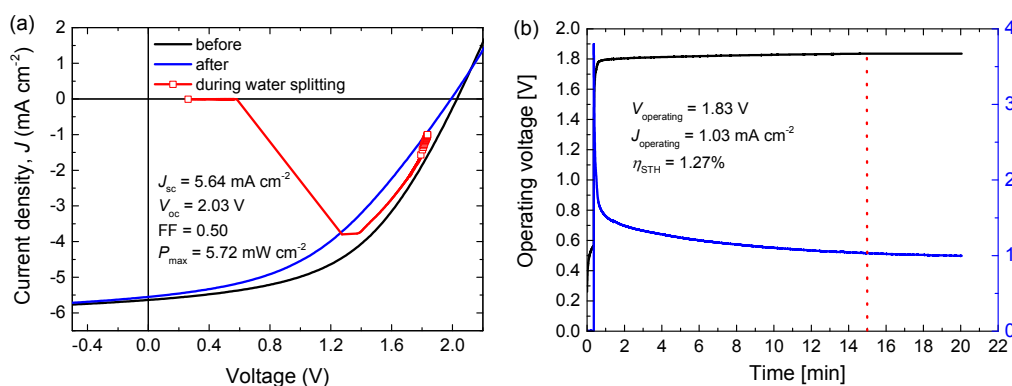
Fig. S1 (a) *J–V* curves of a ~1.2 cm^2 triple junction solar cell connected to Co_3O_4 – NiMoZn catalysts in 0.1 M KBi, before, during and after water splitting measurement of 20 min. (b) Simultaneous measurement of operating voltage and current density of the solar cell during photoelectrochemical water splitting.
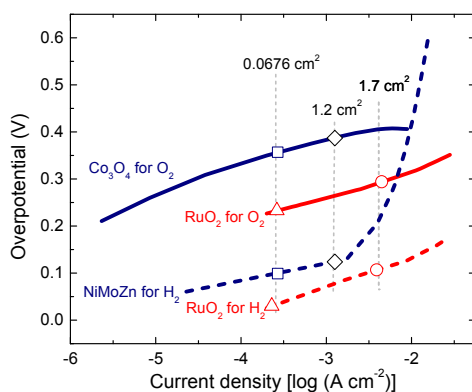

Fig. S2 Tafel plots of RuO_2 in 1.0 M of KOH and of Co_3O_4 and NiMoZn in 0.1 M potassium borate (KBi) at pH 9.2. The markers indicate the expected overpotentials during the operation of the small scale RuO_2/RuO_2 PEC cell (△),the small scale Co_3O_4/NiMoZn PEC cell (□), the large scale RuO_2/RuO_2 PEC cell (○), and the large scale Co_3O_4/NiMoZn PEC cell (◇).

2. Catalyst stability

Stabilities of the catalysts used in the PEC water splitting devices were separately tested with two-electrode measurements. Fig. S3a shows the stability of two RuO_2 catalysts deposited on a Ti plate for oxygen and hydrogen evolution reactions in 1.0 M KOH. Fig. S3b shows data for earth abundant Co_3O_4 and NiMoZn catalysts for oxygen and hydrogen evolution in 0.1 M KBi. The two-electrode measurements were performed at applied potentials of 1.65 V and 1.85 V for 20 min. The applied potentials were selected with respect to the operating potentials of large area artificial leafs. Especially after 15 min, current flow in both electrochemical cells significantly stabilizes.

Nevertheless, RuO_2 catalyst is known to be not completely stable for oxygen evolution reaction as it may oxidize further to one of its other states which are soluble.[1] We have also observed that if a RuO_2 catalyst is continuously kept in 1.0 M KOH for two days without operating, noticeable decrease in its catalytic activity takes place. However if the catalyst is stored in air it quickly restores to its original performance level when contacted again with the electrolyte and enables stable operation up to at least 2 h (Fig. S3c). A detailed study on the stability of RuO2 for hydrogen and oxygen evolution reactions in acid and alkaline media has been reported recently.[2]
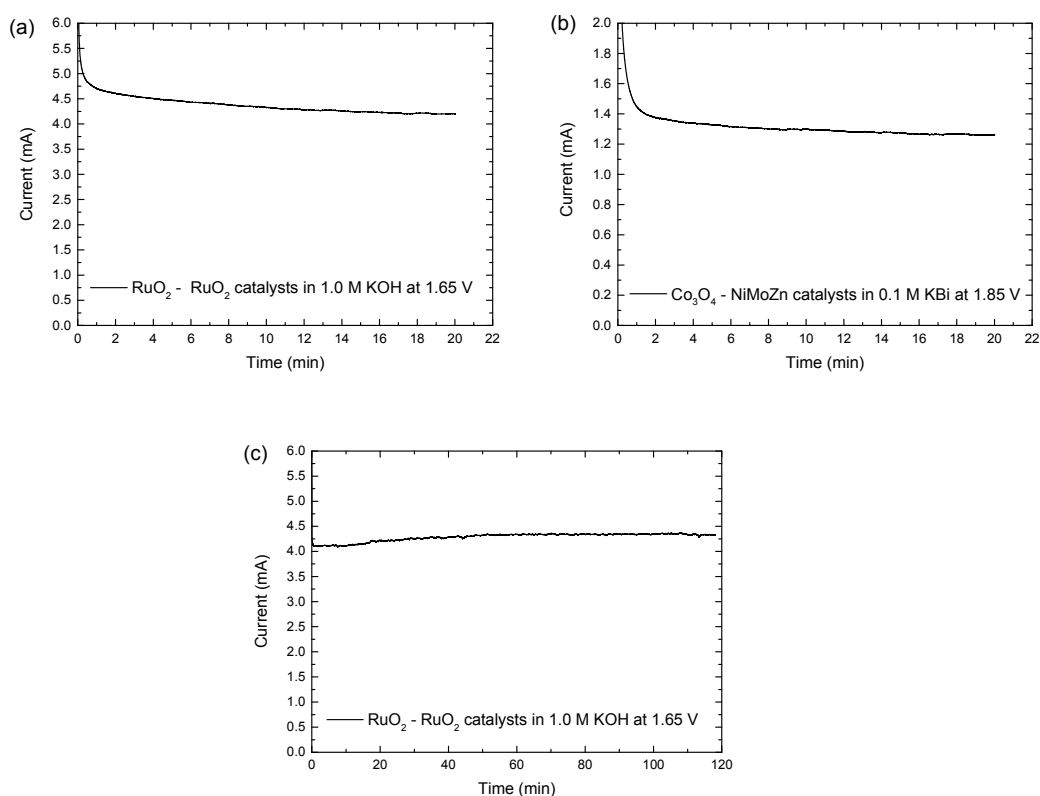

Fig. S3 Stability of (a, c) RuO_2/RuO_2 catalysts in 1.0 M KOH and (b) Co_3O_4/NiMoZn catalysts in 0.1 M KBi for oxygen and hydrogen evolution reactions. Two-electrode water splitting test potentials of 1.65 V (a, c) and 1.85 V (b) were applied for 20 min. (a, b) or 2 h (c). The catalyst used in (c) were stored in air and reached the same activity as freshly prepared catalyst (a) after a short time.

3. Catalyst characterization

3.1 RuO$_2$ on Ti metal

The RuO$_2$ catalyst was characterized using X-ray diffraction (XRD) (Fig. S4) which confirms the formation of RuO$_2$ on Ti metal.
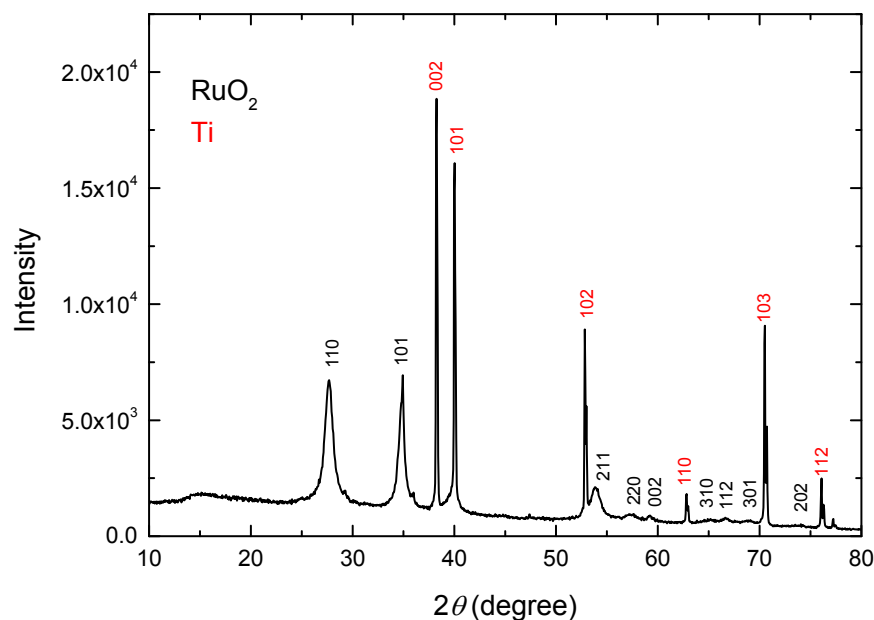
Fig. S4 X-Ray diffraction pattern of RuO$_2$ on Ti metal. The XRD peaks were assigned to RuO$_2$ in a tetragonal crystallographic structure (JCPDS, No.40-1290)[3,4] and Ti metal (JCPDS, No. 44-1294).[5]
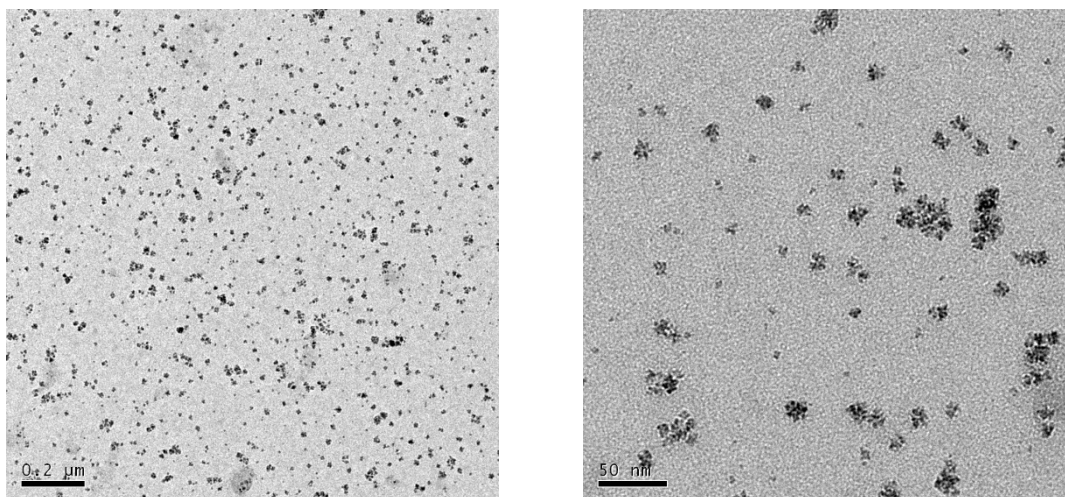
3.2 Co$_3$O$_4$ nanoparticles on ITO

Cobalt oxide nanoparticles were synthesized from a cobalt(II) acetate precursor and obtained as a solution in methanol. To estimate the size of the nanoparticles, the UV-vis spectrum of the nanoparticle solution was measured (Fig. S5). Transitions were observed at 371 and 668 nm. When compared with the transitions at 375 and 675 nm reported in literature for 3 nm Co$_3$O$_4$ nanoparticles, the absorption is slightly blue-shifted indicating that average size of the particles is slightly less than 3 nm.[6] The two transitions have been assigned to O$^{2-} \rightarrow$ Co^{2+} and O$^{2-} \rightarrow$ Co^{3+} transitions.[7,8]
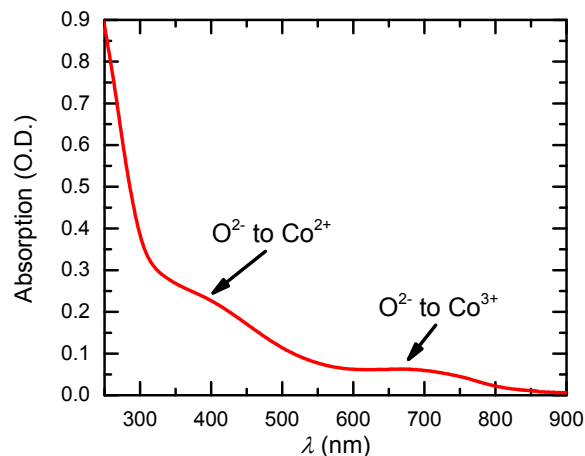
Fig. S5 Absorption spectrum of the Co_3O_4 nanoparticles in methanol.

Transmission electron microscopy (TEM) measurements were carried out to study the geometry and size of the nanoparticles (Fig. S6). TEM shows that the nanoparticles were found to be 3 - 5 nm in size in fair agreement with the UV-vis results. The particle size distribution was narrow.


Fig. S6 TEM images of the prepared Co_3O_4 nanoparticles.

The nanoparticles were deposited onto an ITO coated glass slide to be able to use the nanoparticles as oxygen evolving electrode. To improve the binding to the substrate, the particles were annealed in hot air of 400 to 500 °C for 1 to 2 min. The structure of the nanoparticles at the electrode surface was studied with scanning electron microscopy (SEM), energy-dispersive X-ray (EDX), and XRD. SEM showed that the Co_3O_4 layer on ITO is rough (Fig. S7). AFM revealed height differences of ~100 nm.
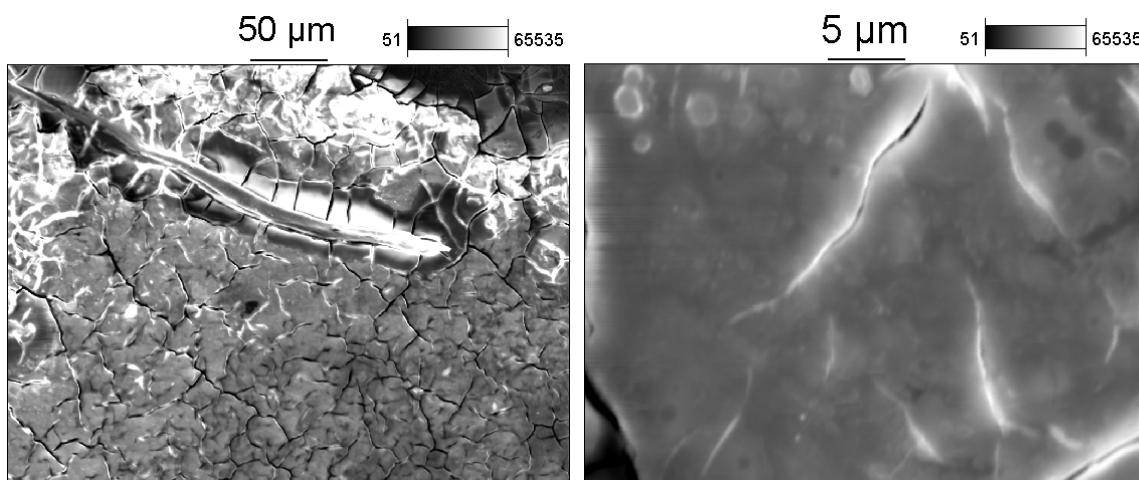
**Fig. S7** Scanning electron microscopy images of a Co₃O₄ nanoparticle catalyst layer.

In the accompanying EDX spectrum (Fig. S8), recorded during the SEM measurements, peaks of silicon, indium, tin, and cobalt, which were expected to be in the spectrum. Also potassium was present, which originates from the KBi electrolyte in which the electrode was tested.
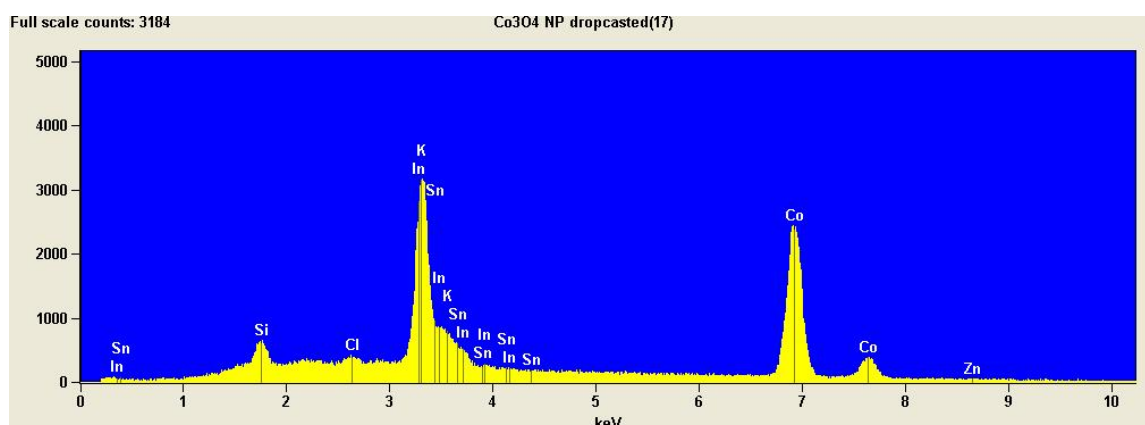
**Fig. S8** EDX spectrum of a Co₃O₄ nanoparticle catalyst layer on an ITO coated glass slide as substrate.

XRD measurements of the powder were consistent with the formation Co₃O₄ on cubic In₂O₃ (Fig. S9). The diffraction peaks of Co₃O₄ are not very clear. The most intense (311) diffraction 36.7° of Co₃O₄ is broad, consistent with the small size of the particles. Of the other expected diffraction peaks the (220) reflection can be identified, but others are not clear.
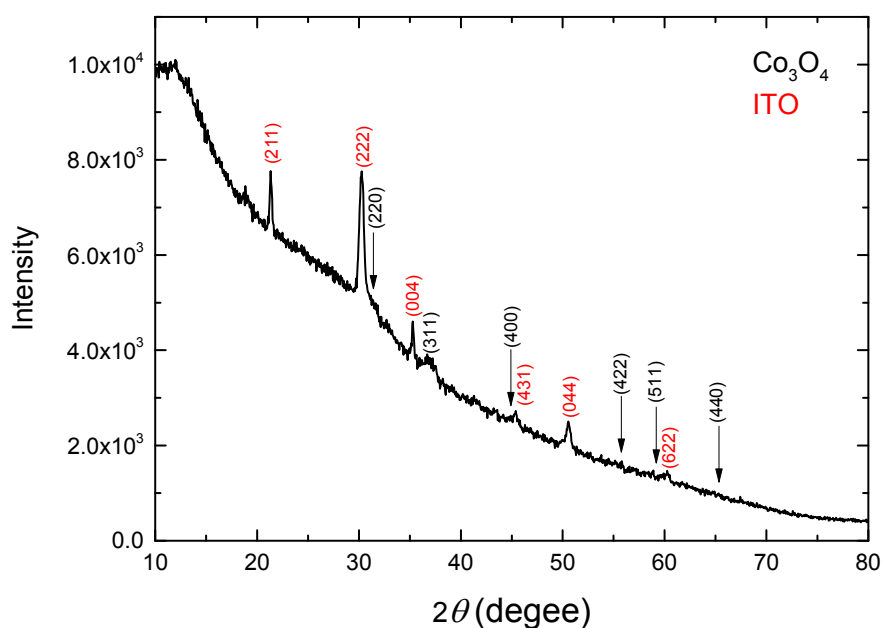
Fig. S9 X-Ray diffraction pattern of Co_3O_4 on ITO (Sn doped In_2O_3). The XRD peaks were assigned to In_2O_3 in a cubic crystallographic structure (JCPDS, No. 65-3170)[9,10] and Co_3O_4 (JCPDS, No. 42-1467, 43-1003). The arrows indicate expected positions for Co_3O_4 for which no clear reflection is observed. Note that the 36.7° (311) peak is the most intense.

3.3 NiMoZn on Ni foil

The successful preparation of a NiMoZn electrode is see from the significant drop of the overpotential of the electrochemically deposited NiMoZn layer on Ni foil by comparing the Tafel plots of NiMoZn and the Ni foil itself.
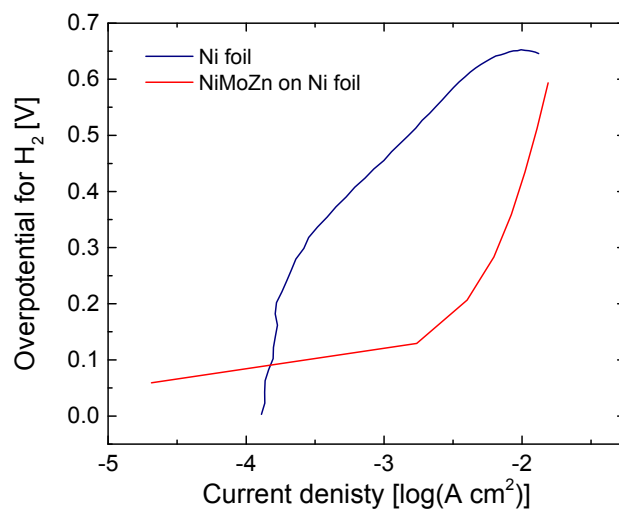
Fig. S10 Tafel plots of NiMoZn and Ni in 0.1 M potassium borate (KBi) at pH 9.2.

4. References

1   K. Juodkazis, J. Juodkazytė, R. Vilkauskaitė, B. Šebeka and V. Jasulaitienė, *Chemija.*, 2008, **19**, 1.

2   S. Cherevko, S. Geiger, O. Kasian, N. Kulyk, J.-P. Grote, A. Savan, B. R. Shrestha, S. Merzlikin, B. Breitbach, A. Ludwig and K. J. J. Mayrhofer, *Catal. Today*, 2015, doi: 10.1016/j.cattod.2015.08.014.

3   D. Rochefort and D. Guay, *J. Alloys Compd.*, 2005, **400**, 257.

4   J. C. Cruz, V. Baglio, S. Siracusano, V. Antonucci, A. S. Aricò, R. Ornelas, L. Ortiz-Frade, G. Osorio-Monreal, S. M. Durón-Torres and L. G. Arriaga, *Int. J. Electrochem. Sci.*, 2011, **6**, 6607.

5   A. W. Hull, *Phys. Rev.*, 1921, **18**, 88.

6   M. Grzelczak, J. Zhang, J. Pfrommer, J. Hartmann, M. Driess, M. Antonietti and X. Wang, *ACS Catal.*, 2013, **3**, 383.

7   J. Pal and P. Chauhan, *Mater. Charact.*, 2010, **61**, 575.

8   R. Xu and H. C. Zeng, *Langmuir*, 2004, **20**, 9780.

9   M. Marezio, *Acta Crystallogr.*, 1966, **20**, 723.

10 Y. Shigesato, Y. Hayashi and T. Haranoh, *Appl. Phys. Lett.*, 1992, **61**, 73.